

## 氧化石墨烯在氧化锌衬底上的电化学还原及其光电性能

李一鸣<sup>1</sup> 陈肖<sup>1</sup> 刘晓军<sup>1</sup> 李文有<sup>1</sup> 贺蕴秋<sup>1,2,\*</sup>

(<sup>1</sup> 同济大学材料科学与工程学院, 上海 201804; <sup>2</sup> 先进土木工程材料教育部重点实验室, 上海 201804)

## Electrochemical Reduction of Graphene Oxide on ZnO Substrate and Its Photoelectric Properties

LI Yi-Ming<sup>1</sup> CHEN Xiao<sup>1</sup> LIU Xiao-Jun<sup>1</sup> LI Wen-You<sup>1</sup> HE Yun-Qiu<sup>1,2,\*</sup>

(<sup>1</sup> School of Materials Science and Engineering, Tongji University, Shanghai 201804, P. R. China;

<sup>2</sup> Key Laboratory of Advanced Civil Engineering Materials, Ministry of Education, Shanghai 201804, P. R. China)

\*Corresponding author. Email: heyunqiu@tongji.edu.cn.

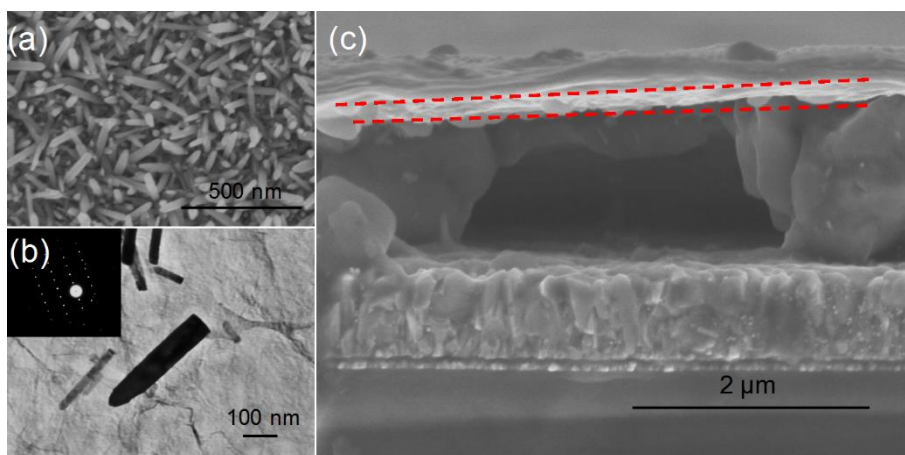


图 S1 (a) ZnO 衬底的表面微观形貌; (b) 从 GO-ZnO 复合膜上剥离得到 GO 样品的 TEM 图像，图中背景的褶皱为 GO 片层形貌。插图为单个 ZnO 纳米柱的选区电子衍射(SAED)斑点; (c) GO 膜的截面形貌

Fig.S1 (a) Micro morphology of the ZnO nanorod array; (b) TEM image of the ZnO nanorods, with the background image of the wrinkled GO flakes. the inset is the selected area electron diffraction (SAED) image of the single nanorod; (c) The cross-sectional view of the GO layer on the GO-ZnO composite film

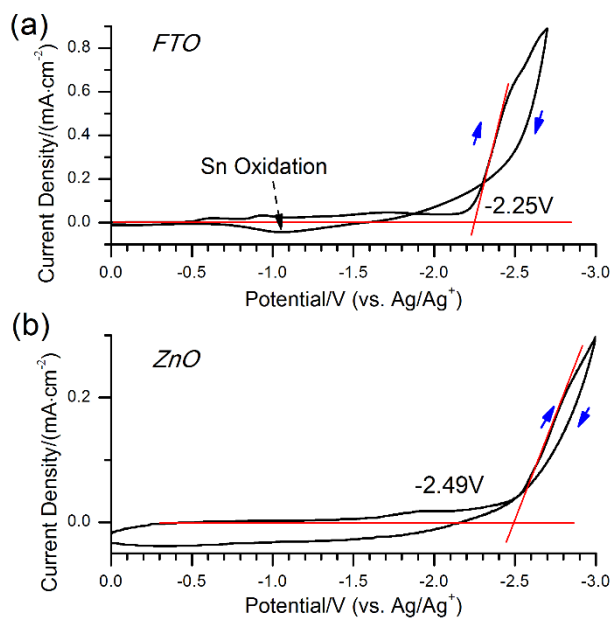


图 S2 (a)和(b)分别为 FTO 玻璃和 ZnO 衬底的循环伏安曲线(扫描速度  $10 \text{ mV}\cdot\text{s}^{-1}$ )

Fig.S2 (a) and (b) are the cyclic voltammograms of the FTO glass and the ZnO film with a scan rate of  $10 \text{ mV}\cdot\text{s}^{-1}$

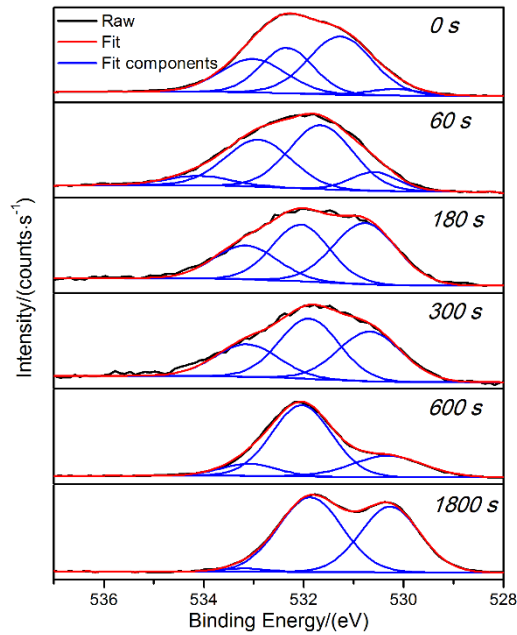


图 S3 不同还原时间复合膜表面的 O1s XPS 图谱, 拟合分峰随结合能增加依次为: ZnO 的 Zn—O 键、GO 羰基 C=O 和羧基 COOH 的混合峰、环氧 C—O—C 键和羟基 C—OH<sup>S1,S2</sup>。注意到与 0s 相比, 60s 图谱中 C—OH 分峰相对于 C—O—C 分峰的含量显著减小; 结合 C1s 分析中, 60s GO 中环氧基含量较 0s GO 显著下降的结论, 可得 60s GO 中的羟基也大幅减少

Fig.S3 The O1s XPS spectra of the GO-ZnO composite films with different reduction time. The fit components are the Zn—O bonds in ZnO, the carbonyl C=O and carboxyl COOH mixed signal, the C—O—C epoxide and the hydroxyl C—OH with increasing order of the binding energy<sup>S1,S2</sup>. The relative intensity of the C—OH peak to the C—O—C peak of the 60s sample is smaller than that of the 0s sample, and the intensity of the C—O—C peak in the 60s sample has dropped a lot from that in the 0s sample as is concluded in the C1s spectra, thus the content of the C—OH bonds in the 60s sample is less than that in the 0s sample

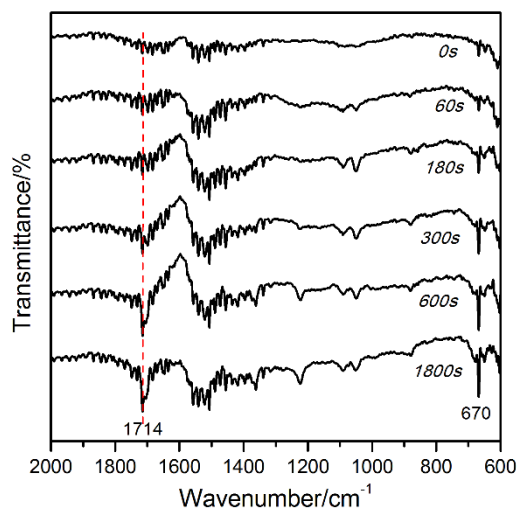


图 S4 各 GO-ZnO 复合膜的 FTIR 衰减全反射透过率图谱

Fig.S4 The FTIR attenuated total reflection transmittance spectra of different GO-ZnO composite films

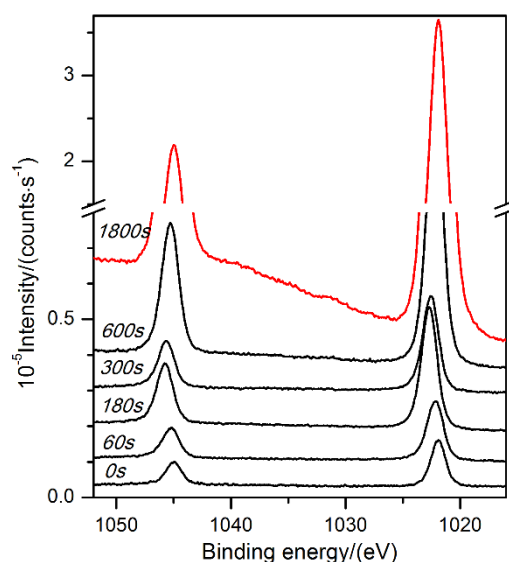


图 S5 不同还原时间复合膜表面的 Zn2p XPS 图谱。随时间变化,各样品 Zn2p 峰的线形未发生显著变化,表明 ZnO 结构在电化学处理过程中一直保持稳定

Fig.S5 The Zn2p XPS spectra of the GO-ZnO composite films with different reduction time. The curved shape remains constant with time, indicating that the chemical structure of ZnO didn't change during the electrochemical process

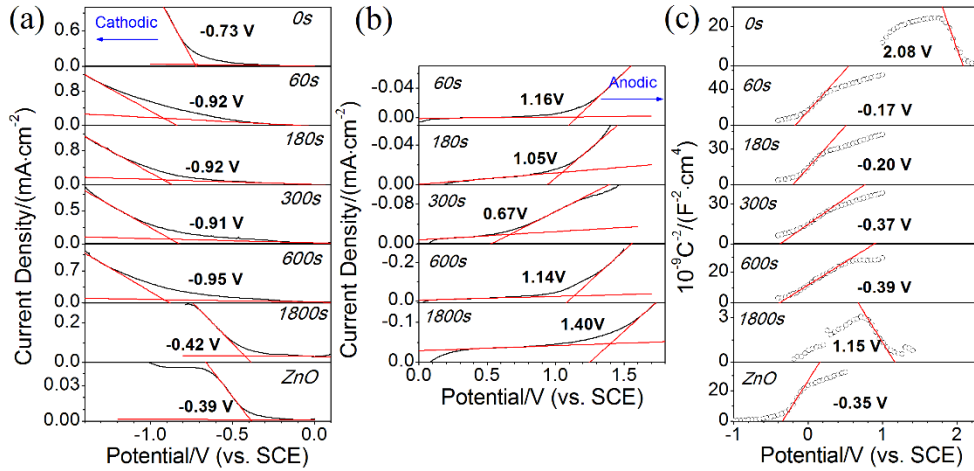


图 S6 样品经过电化学测试得到的(a) 阴极线性扫描伏安(LSV)曲线, (b) 阳极 LSV 曲线和(c) 电化学阻抗(EIS) Mott-Schottky 曲线。测试采用三电极体系, 即样品薄膜为工作电极, Pt 片和 SCE 分别为对电极和参比电极, 在  $0.5 \text{ mol}\cdot\text{L}^{-1}$   $\text{Na}_2\text{SO}_4$  溶液中进行。LSV 测试的扫描速率为  $5 \text{ mV}\cdot\text{s}^{-1}$ , EIS 测试的电位增幅为  $0.01 \text{ V}$ , 测试频率为  $1000 \text{ Hz}$ 。对 LSV 测试, 阴极扫描和阳极扫描中电流出现线性增长的起始电位分别与电极表面半导体的导带底(CBM)和价带顶(VBM)位置对应<sup>S3,S4</sup>。其中在进行阳极 LSV 测试时, 0s 复合膜和 ZnO 膜在曲线出现激增前即由于施加了较大的电位造成电极表面水分子氧化生成  $\text{O}_2$  并使电极破坏, 因此未能得到 VBM 值。对 EIS 测试, 曲线线性段切线与横轴的交点值与电极表面半导体的费米能级对应, 切线斜率则与载流子浓度相关<sup>S4,S5</sup>, 其中斜率符号的正和负分别表示半导体载流子极性为  $n$  型和  $p$  型<sup>S6</sup>

Fig.S6 (a) and (b) are Cathodic and Anodic Linear sweep voltammograms (LSVs) of different samples; (c) Electrochemical impedance spectra (EIS) exhibiting Mott-Schottky characteristics of different samples. The measurements were conducted in  $0.5 \text{ mol}\cdot\text{L}^{-1}$   $\text{Na}_2\text{SO}_4$  solution using a three-electrode configuration with the samples as working electrodes, the Pt foil and the SCE as the counter electrode and the reference electrode, respectively. The LSVs were measured with a scan rate of  $5 \text{ mV}\cdot\text{s}^{-1}$ , the EIS were measured with an amplitude of  $0.01 \text{ V}$  and frequency of  $1000 \text{ Hz}$ . For the LSVs, the crossings of the extrapolations from the initial stage and the abrupt increase stage in pace with the cathodic and anodic scanning could be approximated as the position of the Conduction Band Minimum (CBM) and

Valence Band Maximum (VBM) of the semiconductor on the electrode, respectively<sup>S3,S4</sup>. The results didn't give the VBMs of the 0s GO and ZnO, because the oxygen bubbles were electrochemically generated at the surfaces of the electrodes when scanning to more positive potentials, propagating the films breakdown. For the EIS, the Fermi level and doping concentration of the semiconductor could be determined by the zero-crossing and slope of the tangent from the linear region of the Mott-Schottky plot, respectively<sup>S4,S5</sup>, and the slope direction reflects the carrier type with positive as *n*-type and negative as *p*-type<sup>S6</sup>

#### References

- (S1) Pradhan, D.; Leung, K. T. *Langmuir* **2008**, *24*, 9707. doi: 10.1021/la8008943
- (S2) Yu, Y. H.; Lin, Y. Y.; Lin, C. H.; Chan, C. C.; Huang, Y. C. *Polym. Chem.* **2014**, *5*, 535. doi: 10.1039/c3py00825h
- (S3) Dolai, S.; Dass, A.; Sardar, R. *Langmuir* **2013**, *29*, 6187. doi: 10.1021/la401437r
- (S4) Yeh, T. F.; Teng, C. Y.; Chen, S. J.; Teng, H. *Adv. Mater.* **2014**, *26*, 3297. doi: 10.1002/adma.201305299
- (S5) Boix, P. P.; Ajuria, J.; Etxebarria, I.; Pacios, R.; Garcia-Belmonte, G.; Bisquert, J. *J. Phys. Chem. Lett.* **2011**, *2*, 407. doi: 10.1002/adma.201305299
- (S6) Jang, H.; Kwon, H. J. *Electroanal. Chem.* **2006**, *590*, 120. doi: 10.1016/j.jelechem.2006.02.031